Segmentation of the Left Ventricle from Cine MR Images Using a Comprehensive Approach

Su Huang[1], Jimin Liu[1], Looi Chow Lee[1], Sudhakar K Venkatesh[2], Lynette Li San Teo[2], Christopher Au[2], Wieslaw L. Nowinski[1]

[1]Biomedical Imaging Lab, Singapore Bio-imaging Consortium,
Agency for Science, Technology and Research (A*STAR), Singapore
{huangsu, jmliu, lee_looi_chow, wieslaw}@sbic.a-star.edu.sg
[2]Department of Diagnostic Radiology, Yong Loo Lin School of Medicine,
National University of Singapore, Singapore
dnrskv@nus.edu.sg, lslteo@yahoo.com, christopher_au@nuh.com.sg

Abstract. Segmentation of the left ventricle is important in assessment of cardiac functional parameters. Currently, manual segmentation is the gold standard for acquiring these parameters and can be time-consuming. Therefore, accuracy and automation are two important criteria in improving cardiac image segmentation methods. In this paper, we present a comprehensive approach that utilizes various features of cine MR images and combines multiple image processing methods including thresholding, edge detection, mathematical morphology, deformable model as well as image filtering. The segmentation is performed automatically with minimized interaction to optimize segmentation results. This approach provides cardiac radiologists a practical method for accurate segmentation of the left ventricle.

1. Introduction

Cardiac magnetic resonance images (CMR) has become significantly important in the last decade because of rapid improvement of hardware techniques, computing power, coil design and sequence development. Given the high quality of CMR images, this has surpassed echocardiography which is now no longer the gold standard for cardiac parameters. It is believed that in the future, when cost and time required for image acquisition become comparable to that of echocardiography, CMR will be the primary diagnostic modality in cardiovascular medicine because of its unique versatility and non-invasive nature [1].

Quantitative analysis of clinical parameters such as ejection fraction (EF), left ventricle myocardium mass (MM), and stroke volume (SV) can be obtained by delineation of the left ventricle from cine MR images. These parameters play important roles in cardiac functional assessment, heart failure, cardiomyopathies and congenital heart disease.

The main challenges in left ventricle (LV) automatic segmentation include the following: intensity distribution of cardiac images varies significantly which makes automatic classification or clustering methods ineffective; the shape of the ventricles varies from person to person, hence edge information is inconsistent with the epicardial surface of the left ventricular wall appearing indistinct.

In recent years, quite a number of methods have been proposed for (semi-) automated LV segmentation. To deal with the aforementioned problems, different strategies have been used in these methods include image-driven methods [2, 3], probability atlas [4], dynamic programming [5, 6], fuzzy clustering [7], deformable model [8], active appearance model [9], level set and its variations [10-13], graph cut approach [14, 15]. For a complete review of recent literature describing cardiac segmentation techniques, see [16]. However, fully automatic accurate segmentation of left and right ventricles is still attracting research interest as CMR is

becoming more widely-used and manual segmentation is still a time consuming task for cardiac radiologists.

Our study found that characteristics of cine image from different scans can be quite variable, and hence it is not easy to achieve high accuracy results by applying a single technique automatically. Therefore, we proposed a comprehensive approach by combining several techniques: radial region growing, image edge detection and mathematical morphology. This approach demonstrates robustness in performing the endocardial and epicardial contours segmentation task from cine MR images with achievement of a highly accurate method of automated segmentation. A few other interactions can drastically enhance the results. Firstly, correction of obvious segmentation errors due to poor image quality, or secondly, to enable automated segmentation for images which demonstrate breathing or motion artifacts and do not appear suitable for automated segmentation.

The paper is organized as follows, Section 2 describes details of the segmentation methods, Section 3 presents and discusses the results, followed by Section 4 with conclusion and our future work.

2. Material and Methods

2.1. Image data

The datasets used in this paper are cine steady state free precession (SSFP) MR short axis (SAX) images published by the MICCAI grand challenge on website. 45 cardiac cine MR datasets will be made available for this event in three batches; 15 datasets for training, 15 for testing and 15 for the online contest. Each batch contains 4 heart failure with ischemia (HF-I) cases, 4 heart failure without ischemia (HF-NI) cases, 4 hypertrophy (HYP) cases and 3 normal cases. This paper presents the results of our work based on 30 datasets for the training and testing batches.

All image data were randomly selected from the clinical database from Sunnybrook Health Sciences Centre. All the images were obtained during 10-15 second breath-holds with a temporal resolution of 20 cardiac phases over the heart cycle. Six to 12 SAX images were obtained from the atrioventricular ring to the apex (thickness=8~10mm, FOV=320mm x 320mm, matrix= 256 x 256). (http://smial.sri.utoronto.ca/ LV_Challenge/Data.html)

The goals of this contest are to compare LV segmentation methods by providing an evaluation system, and a database of images and expert contours. Comparing segmentation results across research studies can be difficult due to unspecified differences in the method or implementation of evaluation matrices. This contest provides an open-source code for contour evaluation. Furthermore, the database provides a set of images such that confounding segmentation differences due to image quality or pathology can be eliminated.

2.2. ROI automatic localization

CMR images include the lower chest and upper abdomen. The structures surrounding the heart include the lungs, chest wall/musculature, ribs, liver, gall bladder, spleen, bowel and peritoneal/omental fat. As there are different tissues of different signal intensities, image analysis based on the entire images would be difficult. Several regions of interest (ROI) allocation approaches have been used in previous studies to narrow down the particular area in

the image. For example, in [2], a square area is plotted in the centre of the image as ROI, and in [7], a Hough transform is applied to locate the ROI centre.

We define a region of interest as a circle given that the LV has a circular configuration. Here we describe our method to calculate centre of the ROI circle. In most of the SAX CMR images, the LV centre is near the image centre, because the LV is the region of interest for the cardiac radiologist. In such cases, it is reasonable to assume that the image center falls into the LV blood pool region, although this may not lie exactly in the centre of the LV. We pre-fix a circular region with the diameter equal to half of the image size, rationally the LV falls in this region in most of cases. By calculating the histogram of this region, and applying multilevel Otsu thresholding [17, 18], an approximated threshold value of blood can be determined. Assuming that the image centre falls within the blood pool, we then apply region growing method using the image centre as the seed point. We calculate convex hull based on the region growing result. This convex hull is then used as the initial location of the LV to approximate the ROI circle. Performing a circle fitting on the convex hull with linear least square method[19], we obtain the centre of the blood pool of the LV. Using this centre point as origin, and a diameter that slightly bigger than average diastolic LV (we used 11cm after observed all CMR data we have had), a compact circular ROI is generated for subsequent segmentation process.

In some cases, the image centre may not fall within the blood pool of the LV because of constraints in scanning, the region growing based on assumption of the centre point as seed point may fail. A user interaction is required to set the ROI centre. Since the LV is a circle like object in SAX images, a circle following the mouse cursor is displayed at the centre of image. A user can easily use the mouse to drag the circle so that it looks like concentric circles with the LV. Nevertheless, in the cases that automatic location ROI is not nicely localized, or slices in a phase stack shift seriously (this happens because slices in each phase stack are taken in different breath hold), we also suggest users to define the ROI centre because a precise initial centre of LV in most cases could lead to better segmentation in the following steps.

2.3. Single phase segmentation

In clinical practice, radiologists are interested in the end-diastole (ED) and end-systole (ES) which are the most critical phases in cardiac functional assessment. Determination of the ED and ES phases can be done by visual observation of radiologists or via computer software. Since our method is automated and phase independent, this paper will not cover the ED and ES phase determination.

2.3.1. Endocardial contouring

Given a circular ROI generated in aforementioned steps covering the LV compactly, tissues within the region are more predictable. The LV blood pool and myocardium occupied major volume of the ROI region and other structures such as lung, chest spaces are minimized, hence the intensity distribution is much regular and relatively easy to classify. We observed image intensities in ROI region include various tissues i.e. blood, muscle, fat, lung and chest space. Otsu thresholding[17, 18] is used to classify the intensity of image in ROI to obtain threshold values of blood and muscle.

Using threshold by the Otsu method, a radial region growing is applied to extract the blood pool of the left ventricle. Radial region growing is similar to region growing, however, it is starting from a centre point of a circle, and growing by increasing the radius of the circle pixel by pixel. To ease calculation and illustration, a polar transformation is applied on the region of interest to form a flat image (Fig. 1), while after computing, contours are transformed back from polar coordinates to Cartesian coordinates. Transform image into a polar coordinates

system is an effective method in LV segmentation and it has been used by a few other works[2, 5]. Given the uneven nature of the inner surface of the ventricle due to papillary muscles and chordae tendineae, we compute the convex hull to warp the region growing result so that it includes the papillary muscle region, and then low pass filter of Fast Fourier Transformation on the convex hull to remove the irregular uneven ventricle surface disturbing and form a smooth endocardial contour.

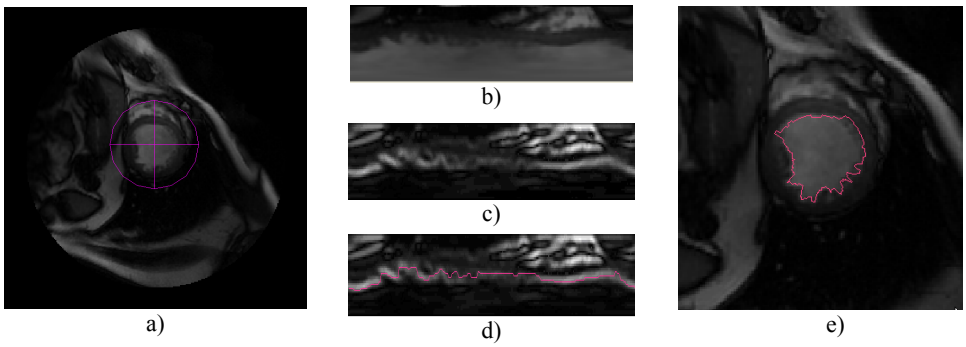

Fig. 1. Segmentation of endocarial contour: a). Region of interest; b) ROI image transformed to polar coordinates; c) Canny filtering result of b); d) edge of LV detected by combined region growing in polar transformed image and edge detection. e) LV transform back to Cartesian coordinates system.

2.3.2. Epicardial contouring

We use canny edge detector [20] on the image within ROI to detect the edge of different tissues. However, LV is surrounded by different structures with different intensity values, therefore, the edge from canny filter is not sufficient to trace the epicardial contours. The intensity thresholds of muscles (myocardium) derived from Otsu method in previous step is also used as combination criteria. The radial region growing is started from the edge of the endocardial. The radial region growing detects both the intensity threshold and the canny filter results to determine the stop criteria. When the radial region growing is stopped, the initial edge of epicardial computed thresholding and canny edging is jaggy, and again, a low pass filter by the Fast Fourier Transformation is applied to produce a well smooth contour that fit to the surface of epicardial.

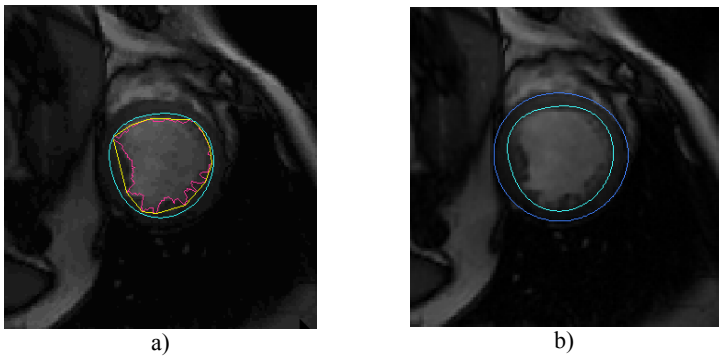

Fig. 2. Segmentation of endocardial and epicarial: a) Endocarial is generated by Fourier transformation from the convex hull of the blood pool edges; b) Epicardial contour produced by radial region growing from endocardial.

2.3.3. Papillary muscles segmentation

Papillary muscles in ventricle occupied a relative significant space in ventricles, therefore these muscles, particularly the two biggest papillary muscles (indicated as P1 and P2) are also need to be delineated and considered when calculating the ventricle eject factors. To outline the papillary muscles, we used the blood's low threshold derived in 2.3.1 again on to the endocardial region. Generally, several dark regions similar to papillary muscles can be identified as candidate regions. We apply a mathematical morphology opening operation on these regions to disconnect weak connections between these candidate regions. The two biggest regions are then selected automatically as papillary muscles P1 and P2. Contours of the two regions are extracted by marching square, a 2-D version of marching cube [21]. The contours finalized by smoothing using Bezier curve fitting.

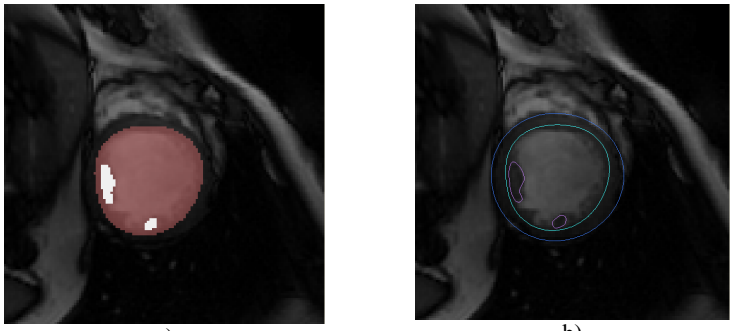

a) b)

Fig. 3. Segmentation of papillary muscles: a). Apply thresholding in the region of endocardial; b). extract contours of papillary muscles.

2.4. Deformable model enhancement in time dimension

Although we aim to a fully automatic segmentation procedure, manual enhancement to the results is sometime inevitable because unforeseeable vast variation in source images quality come from different scanner, operator, and scan conditions. Our design allows users to have final touch to the automatic computed contours in order to output high quality segmentation results. We believe such a system would increase users' confidence to accept the segmentation results. Users' operation and time of finalizing modification to the contours can be minimized by using appropriate contour deforming technology. Ideal situation is when a user makes a modification to segmentation error in contours of one phase, relevant contours in other phases can be corrected accordingly. For instance, a correction to contours in the ED phase can also broadcast to the contours in the phase including ES phase. Since cine MR image is time series motion of heart beat cycle, the contours reflect the deformation of heart beat shape. A deformable model method[22, 23] is suitable to trace correction in other phases given a correction indicated by users in a single phase. Our test shows that this process is efficient and practical in refining segmentation outputs.

3. Results and discussions

Our method has been tested on 30 dataset published by the MICCAI clinical image segmentation grand challenge workshop, including 15 training datasets and 15 validation datasets so far. Further testing will be conducted on the on-site testing and when other data are available.

3.1 Evaluation methods

We used two automatic evaluation measures, average perpendicular distances and overlapping dice Metric, to evaluate our results based on the ground truth contours provided with the test data together by using the evaluation computer software supplied by the Sunnybrooks Health Science Institute, the organizer of the LV segmentation competition. Average perpendicular distance evaluation calculates distance from the automatically segmented contour to the corresponding one manually drawn by expert, averaged over all contour points. Overlapping dice metric calculate the contours areas overlapping proportion between the automatic segmentation results and the ground truth. Besides automatic evaluation, visual evaluation has also been conducted by experienced cardiologists based on their general impression on the results contours.

3.2 Evaluation results and discussions

The average distance compare to the ground truth contours provided by Sunnybrooks Health Science Centre is listed in table 1, using the evaluation software provided by the same institute. The perpendicular distances of our results contours to ground truth is about 2 mm for both endocardial and epicardial contours. This is comparable to other methods developed in recently [2, 12] although they are not directly comparable because difference in data and ground truth. Considering inter-operator and intra-operator segmentation errors, the automatic segmentation results should be acceptable clinically.

Table 1. Contour accuracy in terms of average distance and dice matrix of all cases(mean_value ± standard_deviation).

	Studies	Endocardial distance (mm)	Epicardial distance (mm)	Endocardial dice metric	Epicardial dice metric
Training Data	15	2.03±0.34	2.28±0.42	0.90±0.04	0.93±0.02
Validation Data	15	2.10 ±0.44	1.95±0.34	0.89±0.04	0.94±0.01
Total Data	30	2.06±0.39	2.11±0.41	0.89±0.04	0.93±0.02

Table 2 presented the results of average distances to the same ground truth contours categorized by pathology of subjects. The results of heart failure groups appear very slightly better but not very significant. That means our approach is not sensitive to pathology.

Table 2. Contour accuracy in terms of average distance and dice metric categariezed by subjects syndromes (mean_value ± standard_deviation).

Group	Studies	Endocardial distance	Epicardial distance	Endocardial dice metric	Epicardial dice metric
HF-I	8	1.82±0.33	2.02±0.51	0.93±0.01	0.94±0.01
HF-NI	8	2.00±0.35	2.07±0.46	0.92±0.01	0.94±0.01
HYP	8	2.27±0.42	2.13±0.23	0.86±0.04	0.93±0.01
Normal	6	2.19±0.33	2.28±0.44	0.87±0.03	0.92±0.01

Finally, results contours of the validation data (15 studies) are also been visually evaluated by experienced cardiologists at Sunnybrook Health Sciences Centre (Kim Connelly and Gideon Paul). Results are rated with 4 points scale (1: excellent, little correction required; 2: Good, over 50% of contours are acceptable; 3: Poor, less than 50% of the contours are acceptable; and 4: Not usable). The visual evaluation results are shown in Table 3. In the 15 results been evaluated, 11 of them (73%) are rated 1, and 4 of them (27%) are rated 2. This evaluation result, on the other hand, further confirms our segmentation approach generated acceptable results to clinicians.

Table 3. Visual evaluating results. For group HF-I, all the result are visually excellent. Other groups have some small problems but all are in good categary, which means most of contours segmented are acceptable to experienced cardiaologists, only small corrections are needed.

Group	Studies	Rate 1	Rate 2	Rate 3	Rate 4	Average
HF-I	4	4	0	0	0	1
HF-NI	4	3	1	0	0	1.25
HYP	4	2	2	0	0	1.5
Normal	3	2	1	0	0	1.33
Total	15	11	4	0	0	1.27

Nevertheless, the remarks from the visual evaluation reviewers underline the most problematic issue is in the Left Ventricle Outflow Tract (LVOT) area, which is a generic problems to most LV segmentation methods. We need to spend much effort on this issue in our future work.

4. Conclusion and future work

We have developed a comprehensive segmentation approach to segment the left ventricle from cine MR images by using a processing pipeline of image transformation, thresholding, region growing, edge detection and image filtering technologies. Endocardial and epicardial contours as well as two papillary muscles are delineated automatically. Testing results on the data randomly selected from clinical images by Sunnybrook Health Sciences Centre demonstrated that our comprehensive approach of the left ventricle segmentation is a feasible and fast method for cardiac cine MR image segmentation. Its accuracy is comparable to other methods published recently.

Several areas still can be improved and enhanced to increase the accuracy of segmentation. First, automatic allocation of the centre and radius of circular ROI can be optimized to achieve better result in fully automatic segmentation. Meanwhile, end diastolic phase and end systolic phase automatically determination is a nice function to be integrated into the approach. We also found that in some situations that image intensity of LV blood pool is not nicely distribute due to blood flow motion effect, adaptive measure can be added into the region growing method to increase the accuracy of endocardial contours. More intelligent method, for instance, knowledge driven and feature driven techniques can be implemented to trace LV contours from cine MR images with high accuracy.

Acknowledgments

We thank Sunnybrook Health Sciences Centre for making their clinical image data, ground truth contour data and evaluation software accessible to us.

We gratefully acknowledge funding for this research by the Biomedical Research Council, Agency for Science, Technology and Research, Singapore.

Reference

1. Selvanayagam, J.B., et al., *Cardiovascular Magnetic Resonance: Basic Principles, Methods and Techniques*, in *Cardiac CT, PET and MR*, V. Dilsizian and G.M. Pohost, Editors. 2007. p. 28-68.
2. Lu, Y., et al., *Segmentation of Left Ventricle in Cardiac Cine MRI: An Automatic Image-Driven Method*, in *Med Image Comp Comp Assist Interv*, H.D. N. Ayache, and M. Sermesant, Editor. 2008, LNCS. p. 339-346.

3. Chris A. Cocosco, W.J.N., Thomas Netsch, Evert-jan P.A. Vonken, Gunnar Lund, Alexander Stork, Max A. Viergever,, *Automatic image-driven segmentation of the ventricles in cardiac cine MRI.* Journal of Magnetic Resonance Imaging, 2008. **28**(2): p. 366-374.
4. Lorenzo-Valdes, M., et al., *Segmentation of 4D cardiac MR images using a probabilistic atlas and the EM algorithm.* Medical Image Analysis, 2004. **8**(3): p. 255-265.
5. Pednekar, A., et al., *Automated left ventricular segmentation in cardiac MRI.* Biomedical Engineering, IEEE Transactions on, 2006. **53**(7): p. 1425-1428.
6. Uzümcü, M., et al., *Time continuous tracking and segmentation of cardiovascular magnetic resonance images using multidimensional dynamic programming.* Invest Radiol, 2006. **41**(1): p. 52-62.
7. Rezaee, M.R., et al., *A multiresolution image segmentation technique based on pyramidal segmentation and fuzzy clustering.* Image Processing, IEEE Transactions on, 2000. **9**(7): p. 1238-1248.
8. Kaus, M.R., et al., *Automated segmentation of the left ventricle in cardiac MRI.* Medical Image Analysis, 2004. **8**(3): p. 245-254.
9. Mitchell, S.C., et al., *Multistage hybrid active appearance model matching: segmentation of left and right ventricles in cardiac MR images.* Medical Imaging, IEEE Transactions on, 2001. **20**(5): p. 415-423.
10. Paragios, N., *A level set approach for shape-driven segmentation and tracking of the left ventricle.* Medical Imaging, IEEE Transactions on, 2003. **22**(6): p. 773-776.
11. Fradkin, M., et al., *Comprehensive Segmentation of Cine Cardiac MR Images*, in *Med Image Comp Comp Assist Interv*. 2008. p. 178-185.
12. Lynch, M., O. Ghita, and P.F. Whelan, *Segmentation of the Left Ventricle of the Heart in 3-D+t MRI Data Using an Optimized Nonrigid Temporal Model.* Medical Imaging, IEEE Transactions on, 2008. **27**(2): p. 195-203.
13. Ayed, I.B., et al., *Left Ventricle Tracking Using Overlap Priors*, in *Med Image Comp Comp Assist Interv*. 2008. p. 1025-1033.
14. Boykov, Y. and M.-P. Jolly, *Interactive Organ Segmentation Using Graph Cuts*, in *Medical Image Computing and Computer-Assisted Intervention - MICCAI 2000*. 2000. p. 276-286.
15. Xiang, L., B. Cowan, and A. Young. *Model-based Graph Cut Method for Segmentation of the Left Ventricle*. in *Engineering in Medicine and Biology Society, 2005. IEEE-EMBS 2005. 27th Annual International Conference of the*. 2005.
16. Frangi, A.F., W.J. Niessen, and M.A. Viergever, *Three-dimensional modeling for functional analysis of cardiac images, a review.* Medical Imaging, IEEE Transactions on, 2001. **20**(1): p. 2-5.
17. Otsu, N., *A Threshold Selection Method from Gray-Level Histograms.* Systems, Man and Cybernetics, IEEE Transactions on, 1979. **9**(1): p. 62-66.
18. Liao, P.S. and T.S.C.P.C. Chung, *A Fast Algorithm for Multilevel Thresholding.* J. Inf. Sci. Eng., 2001. **17**(5): p. 713-727.
19. Coope, I.D., *Circle fitting by linear and nonlinear least squares.* J. Optim. Theory Appl., 1993. **76**(2): p. 381-388.
20. Canny, J., *A Computational Approach to Edge Detection.* Pattern Analysis and Machine Intelligence, IEEE Transactions on, 1986. **PAMI-8**(6): p. 679-698.
21. Lorensen, W.E. and H.E. Cline, *Marching Cubes: A high resolution 3D surface construction algorithm.* Computer Graphics, 1987. **21**(4): p. 163-169.
22. Kass, M., A. Witkin, and D. Terzopoulos, *Snakes: active contour models.* International Journal of Computer Vision, 1988. **1**(4): p. 321-331.
23. Liu, J., S. Huang, and W.L. Nowinski, *A hybrid approach for segmentation of anatomic structures in medical images.* International Journal of Computer Assisted Radiology and Surgery, 2008. **3**(3-4): p. 213-219.